INTERNATIONAL ATOMIC ENERGY AGENCY
UNITED NATIONS EDUCATIONAL, SCIENTIFIC AND CULTURAL ORGANIZATION

INTERNATIONAL CENTRE FOR THEORETICAL PHYSICS
34100 TRIESTE (ITALY) - P.O.B. 586 - MIRAMARE - STRADA COSTIERA 11 - TELEPHONE: 2240-1
CABLE: CENTRATOM - TELEX 460392-I

SMR/291 - 40

SPRING COLLEGE IN CONDENSED MATTER
ON
"THE INTERACTION OF ATOMS & MOLECULES WITH SOLID SURFACES"
(25 April - 17 June 1988)

ELEMENTARY CHEMICAL PROCESSES ON SURFACES AND HETEROGENEOUS CATALYSIS
(Lectures III, IV & V)

Andrew HAMNETT
Inorganic Chemistry Laboratory
University of Oxford
South Parks Road
Oxford OX1 3QR
UK

---

1)

Lecture 3

The Chemisorbed Layer

We have seen that physisorption and chemisorption are clearly linked, and that the transfer from the one state to the other may take place more or less rapidly depending on the balance of rate constants as discussed in the previous lecture. We now turn to a consideration of the adsirbed layer on a variety of substrates. The behaviour of the layer will differ quailitatively according to the energy of interaction between adsorbed species and we can treat this at the semi-quantitative level using the Bragg-Williams approximation. We assume

(i) that adsorbed atoms are localised on well-defined and equivalent sites of the substrate
(ii) that interactions are restricted to nearest neighbours
(iii) that there is a random distribution of adsorbed atoms on substrate sites [corresponding to the theory of *regular solutions*]

Let θ be the coverage, E_s the potential energy of a surface site and w the energy of interaction between adsorbed nearest-neighbours such that $w > 0$ corresponds to repulsion and $w < 0$ to attractive interactions. If z is the number of nearest neighbours in the layer:

$$\mu_s = E_s + zw\theta + kT\ln\{\theta/(1-\theta)\} - kT\ln\{f_{vib}(T)\}$$

where $f_{vib}(T)$ is the vibrational partition function (p.f.) of an adsorbed atom. If there is equilibrium between the surface and gas-phase atoms, and, in the gas phase,

$$\mu_g = \mu_g^0 + kT\ln\{p\}$$

where p is the gas pressure, then

$$p = [\theta/(1-\theta)]\alpha(T)\exp[(E_s + zw\theta)/kT]$$

This result is termed the Fowler-Guggenheim isotherm[40], and it clearly reduces to the well-known Langmuir isotherm:

$$p = \theta/[K(1-\theta)]$$

in the limit that $w \to 0$. If $p_{1/2}$ is the pressure of gas corresponding to $\theta = 1/2$, then a plot of $\ln\{p(\theta)/p_{1/2}\}$ *vs.* θ will have the form shown in fig.[21] for different values of w. It will be aseen that for $zw/kT < -4$, the isotherm shows a double loop characteristic of a phase transition. Physically, in this region, the layer consists of a dilute phase of local coverage θ_A which co-exists with a dense phse of coverage θ_B. The relative proportions of these two phases are determined by the total coverage θ as calculated from the Fowler-Guggenheim isotherm.

Although this model does have qualitative appeal, quantitative agreement between experment and theory is poor, even when single-crystal surfaces are used since

(i) the low coverage phase is extremely sensitive to the presence of impurities and defects on the surface

(ii) particularly in the case of chemisorption, thermodynamic equilibrium is hard to achieve save at high temperatures and low pressures
(iii) adsorption on a particular site may profoundly modify the value of E_s not only for nearest neighbour sites but for sites several interatomic distances away.

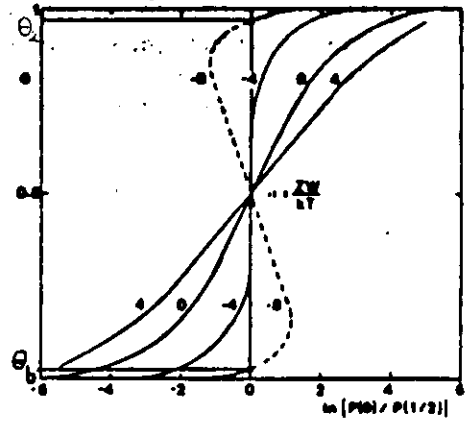

Fig.[21]. Fowler-Guggenheim Isotherm for Adsorption. The figures labelling the curves are values of zw/kT.

A paradigmatic example of a phase transition of the above type is found for the chemisorption of S on Ag(100). By using mixtures of H_2S and H_2 at temperatures in the region of 200°C, two phases could be identified and characterised[41]. A high coverage-density phase has sulphur coordinated to two silver atoms and a low coverage-density phase has sulphur coordinated to four silver atoms. Both these phases are present between he limiting coverages θ_A and θ_B, and can be "frozen in" by rapid quenching under vacuum.

In general, the assumption of a constant coverage-independent value of E_s is a severe limitation as indicated above, even on single-crystal substrates. Even if we restrict ourselves to monolayer adsorption, the existence of a range of E_s values will lead to a modified form of the adsorption isotherm. The simplest case will be found if the heat of adsorption declines linearly with θ, such that

$$-\Delta H_{ads} = -\Delta H_o(1 - \beta\theta)$$

(since $\Delta H_{ads} < 0$). Then, approximately

$$\theta = -(RT/\beta\Delta H_o)\ln\{\kappa p\}$$

where κ is a constant related to the enthalpy of adsorption. This is termed the Temkin isotherm. If the heat of adsorption declines logarithmically with coverage over a range of (intermediate) θ values, such that

$$-\Delta H_{ads} = -\Delta H' \ln(\theta)$$

then, approximately, over the same intermediate range of θ values

$$\theta \sim kp^{1/n}$$

where $n > 1$ and is independent of θ. This is termed the Freundlich isotherm, and is frequently found for θ values between 0.2 and 0.8.

These two isotherms have been used and discussed extensively[6,26,42]. It must be emphasised that not only are data often insufficiently precise to distinguiish the various isotherms, but the fact that one of them might appear to fit the data reasonably well cannot be taken as evidence for the veracity of the underlying assumptions.

Energetics of Chemisorption

The values of $-\Delta H_{ads}$ show wide variation both for gas and substrate. In general, the order of $-\Delta H_{ads}$ for gases over a wide range of substrates follows the order $O_2 > C_2H_2 > C_2H_4 > CO > H_2 > CO_2 > N_2$ with the notable exception of Au, which does not adsorb O_2. Metals may be classified, following Bond[26], into seven classes according to their ability to chemisorb gases, and this classification is given in Table 3.1

Table 3.1

Class	Metal or group in periodic table[a]	Gases						
		O_2	C_2H_2	C_2H_4	CO	H_2	CO_2	N_2
A	Groups IVA, VA, VIA $VIIIA_1$	Y[b]	Y	Y	Y	Y	Y	Y
B_1	Ni, Co	Y	Y	Y	Y	Y	Y	N
B_2	Rh, Pd, Pt, Ir	Y	Y	Y	Y	Y	N	N
B_3	Mn, Cu	Y	Y	Y	Y	Y/N	N	N
C	Al, Au	Y	Y	Y	Y	N	N	N
D	Group IA	Y	Y[c]	N	N	N	N	N
E	Mg, Ag, Group IIB In, Groups IVB, VB	Y	N	N	N	N	N	N

[a]Group IVA: Ti,Zr, Hf; VA: V, Nb, Ta; VIA: Cr, Mo, W; IA: Li, Na, K
IIB: Zn, Cd; IVB: Si, Ge, Sn, Pb; VB: As, Sb, Bi.

[b]Y: strong chemisorption; Y/N: weak chemisorption; N: no observable chemisorption.

[c]Ethyne adsorbs on IA metals as $2M + C_2H_2 \rightarrow M^+C_2H^- + MH$

Examination of Table 3.1 shows that transition metals are strong adsorbers whereas main-group metals are not. It has been suggested that

unpaired d-electrons are necessary to stabilise the precursor state and therefore to permit transition to a stongly bonded chemisorbed state to take place without a high activation energy.

If we compare the enthalpies of adsorption and those of oxide formation, then the pattern is shown in fig.[22].

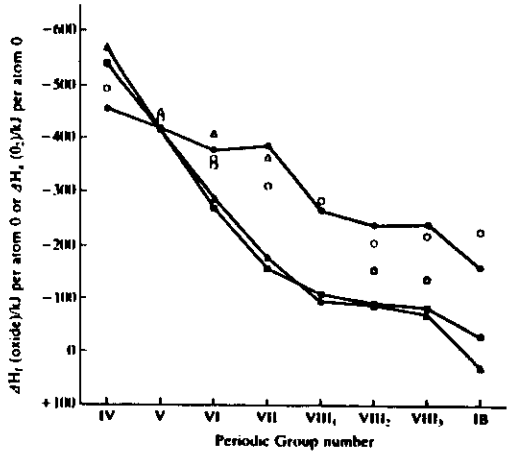

Fig.[22]. Enthalpies of formation of oxides (filled points) and of chemisorption on metals (open points) as a function of Periodic group number. Circles: first transition series; squares: second transition series; triangles: third transition series.

The first point to note is that there is a remarkable parallelism of the data for the first transition series. For the second and third rows, the bulk oxides are significantly less stable than the adsorbed oxygen layers, reflecting possibly the very high atomisation energies in this part of the periodic table. A similar situation is found in the nitrides, though data is less complete, but for hydrogen, the data for bulk hydrides is too sparse for a meaningful comparison.

For the adsorption of CO, the enthalpies of adsorption are shown in fig.[23]. Again, this data shows a semi-quantitative similarity to the bond enthalpy data for the M–CO bond in metal carbonyls, at least in the later transition metals. However, the early transition metals show a much higher value of $-\Delta H_{ads}$ than bond enthalpy, a phenomenon associated with the probable dissociative chemisorption of CO on groups IV - VI.

A very similar set of data is available for the adsorption of CO_2.

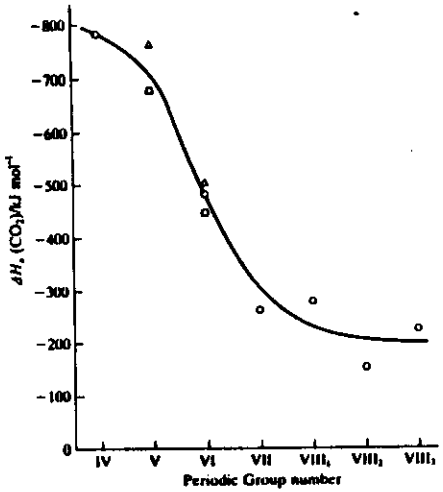

Fig.[23]. Enthalpies of chemisorption of carbon monoxide as a function of Periodic Group Number. Symbols as for fig.[22].

Adsorption on non-elemental Materials

The study of the adsorption of gases on metals has been central to the development of our theoretical understanding of catalysis, but it is a fact that an ever-increasing number of industrial catalysts are based on oxides, sulphides and pnictides. Not only binary, but ternary and quaternary species are known, and a major problem in modern catalytic studies is to establish the surface composition of often complex catalyst formulations. A second difficulty is that the surface composition may alter as a result of exposure to the gas mixture to be catalysed, and the third problem is that even if single crystals of known surface composition can be synthesised, the much higher surface potentials associated with ionic or partly ionic materials will lead to a much higher sensitivity of chemisorption to crystal face and to the presence of kink and step sites on the surface.

(A) Surface Composition

If surface and bulk compositions differ in the intrinsic material, we have a phenomenon known as *segregation*. Simple segregation may be treated by an extension of the statistical treatment given at the beginning of this lecture. In dilute solution, the chemical potential of a dissolved atom will take the form:

$$\mu_b = E_b + kT\ln(x) - kT\ln\{f_b(T)\}$$

where x is the mole fraction, E_b the potential energy of a dissolved atom, and $f_b(T)$ the associated change in vibrational partition function associated with the presence of the atom. Equating this to μ_s gives a relationship between x and θ very similar to the Fowler-Guggenheim isotherm:

$$x = [\theta/(1-\theta)]\alpha'(T)\exp[(zw\theta - E)/kT]$$

where $E = E_b - E_s$.

Perhaps the simplest example of this kind is found for Nickel metal containing a low (< 1%) concentration of carbon in the *bulk* phase. At high temperature ($T > T_s$), the surface coverage of carbon on Ni(111) is low, and appears to approximate the bulk concentration, as shown in fig.[24].

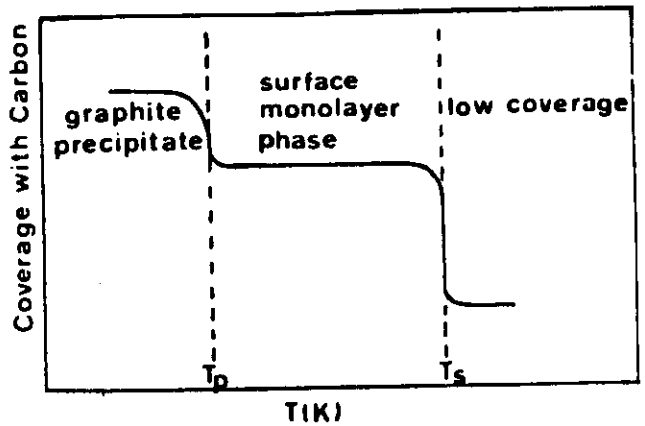

Fig.[24]. Schematic equilibrium temperature dependence of carbon coverage on the (111) surface of a carbon-doped nickel single crystal. A phase transition from a low coverage to a condensed state takes place at the segregation point T_s. Graphite precipitation starts at T_p[43,44].

At lower temperatures, the C-C interactions on the surface become dominant and a phase transition takes place to yield a monolayer phase. At a lower temperature still, bulk graphite forms at the surface. This remarkable behaviour has been analysed by Blakely and co-workers[43,44] who conclude that the binding energy of carbon in the monolayer phase is some 10% higher than E_b.

A similar result has been reported by Egdell and coworkers for antimony segregation onto $SnO_2(001)$[45]. It is well known that SnO_2 containing *ca.* 3% Sb shows both metallic conductivity and transparency to visible light. This remarkable combination of properties has attracted the attention of many scientists, including catalyst chemists, and early results in the field of catalysis were interpreted in terms of the electronic theory of chemisorption. However, Egdell demonstrated clearly that following equilibration at high temperatures, the surface coverage of Sb was far higher than the bulk composition value would suggest, being close to 50%.

In both the Ni(111)/C and $SnO_2(001)$/Sb cases, geometrical models showed that a stable chemical form could exist. For Ni(111)/C, an excellent fit of substrate and ordered hexagonal carbon layer was demonstrated, and the importance of this is pointed up by the fact that other Ni faces may exhibit quite different behaviour, including showing no detectable segregation of carbon to the surface. In the SnO_2 case, Sb is present as Sb(V) in the bulk but apparently as Sb(III) at the surface, and the stereochemical effect of the lone pair is believed to be of importance in stabilising adsorption at low coordination-number surface sites.

An interesting example of segregation is found for the mixed oxides $CoO-Cr_2O_3$ and $NiO-Cr_2O_3$. Measurements of the activation energy for surface diffusion of cations and XPS data both indicate a considerable segregation of Cr to the surface - even in samples containing less than 1% Cr_2O_3[46]. The surface diffusion measurements are, in fact, consistent with the formation of a spinel phase $CoCr_2O_4$ at the surface. Similar conclusions have also been drawn for the $NiO-Cr_2O_3$ case, and SIMS data reveal that the surface composition relaxes towards that of the bulk over an extremely narrow range of 10-20 monolayers[47].

(B) Dynamic Composition Effects

Many transition-metal oxides are effectively non-stoicheiometric, and their composition will depend on the partial pressure of oxygen in the gas phase. Two types of behaviour are found, depending on whether the metal ion has an easily accessible higher or lower oxidation state. In the first case, oxygen is gained on heating the crystal in O_2, usually by formation of metal vacancies as:

$$1/2\,O_2 \longrightarrow V_M + O_O$$

$$M_M + V_M \longrightarrow M_M^{\cdot} + V_M^{\cdot}$$

a situation found for NiO and CoO. In the second case, oxygen is lost either by formation of *oxygen vacancies*:

$$O_O \longrightarrow V_O + 1/2\,O_2$$

as in TiO_2 (at low vacancy concentration), or by formation of metal interstitials:

$$MO \longrightarrow M_i + V_O + 1/2\,O_2$$

as found for ZnO. In certain cases, at higher oxygen-vacancy concentrations, the vacancies may *order* to form shear planes, and examples include TiO_2 and V_2O_5.

The significance of these vacancies is twofold. First, they may confer electronic conductivity on the oxide and this permits redox reactions to take place on the surface. Secondly, they may also show a marked tendency to segregate to the surface under certain conditions. In addition, dynamic processes may result in the accommodation of defects by chemical reactions: thus, hydrogen is believed to adsorb heterolytically on reducible oxides as:

$$H_2 + M^{2+} + O^{2-} \longrightarrow H\text{-}M^{+} + O\text{-}H^{-}$$

Heating will cause the formation of V_O and reduced metal species. Similar effects are found for CO adsorption as

$$CO + M^{2+} + O^{2-} \longrightarrow M^{o} + CO_2$$

In a similar way, O_2 may adsorb on oxidisable oxides as:

$$2Ni^{2+} + O_2 \longrightarrow 2(O^{-}..Ni^{3+})$$

and high surface coverages of O^{-} may result.

More subtle effects may involve the actual reconstruction of the surface. One example is that of $Cu_2^{I}Mo_3^{VI}O_{10}$. This is a selective oxidation catalyst that converts but-1-ene to butadiene but its activity and selectivity can be p[rofoundly modified by exposing the surface to pulses of pure oxygen. It has been shown that this is associated with the formation of clusters of $Cu^{II}Mo^{VI}O_4$ which, on re-reduction to the parent compound, have a very high activity for the selective oxidation process. Of course, this process may result in the disintegration of the catalyst over a period of time, and this may make it quite unsuitable for technological operation.

The central point here is that the state of the surface during dynamic operation may be completely different from that expected on the basis of the known stoichiometry of the bulk catalyst, and that the state of the surface may have a profound influence on the course of a particular reaction.

(C) Influence of surface geometry and structure

Although speculation on the importance of surface geometry has a long history (see *eg* ref.[48]), the first direct answer was given in an elegant series of papers by samorjai and co-workers[49]. In these experiments, dehydrogenation and hydrogenolysis were studied on a wide variety of crystal planes of a single-crystal platinum substrate. High index planes contain controlled concentrations of kink and step sites, and these can be monitored by LEED. The rate of hydrogenolysis was found to depend strongly on the concentration of steps and knks, and it was clear that the reaction must inviolve low-coordinated platinum atoms present at these sites. By contrast, dehydrogenation does not appear to depend on such sites and apparently takes place on the terraces.

Within the selective oxidation field, equally interesting data have been provided by Gasiov and Machej[49] for the oxidation of *o*-xylene on V_2O_5. High conversion to phthalic anhydride was found for crystallites exposing the (001) face, which consists of V=O units arranged perpendicular to the surface plane. However, if the crystallites expose the (110) face, at which shear planes may nucleate and oxygen removed, therefore, more easily, complete oxidation to Co and CO_2 becomes the favoured route. A similar phenomenon was observed on MoO_3 for the oxidation of methanol to HCHO or MeOMe[50].

40. R.H. Fowler and E.A. Guggenheim
"Statistical Thermodynamics", C.U.P., 1939, p.429
41. P. Rousseau, P. Delescluze, F. Delamare, N. Barbouth and J. Oudar
Surf. Technol. 7 (1978) 91
42. *Adamson*

43. M. Eizenberg and J.M. Blakely
Surf. Sci. 82 (1979) 493
44. J.M. Blakely
Crit. Rev. Sol. State Mat. Sci. 7 (1978) 333
45. R.G. Egdell

46. J. Nowotny, I. Sikora and J.B. Wagner
J. Amer. Ceram. Soc. 65 (1982) 192
47. J. Haber in "Surface Properties and Catalysis by Non-Metals"
ed. J.P. Bonnelle, publ. D. Reidel, New York, 1983, p.1
48. G. Rienecker
Ang. Chem. 69 (1957) 545
49. G. Samorjai
Catal. Rev. 18 (1978) 173, and references therein.
50. J.M. Tatibouet and J.P. Germain
J. Catal. 72 (1981) 375

Lecture 4

I. More complex adsorption problems

The adsorption of CO on transition metal substrates has been extensively studied, and some degree of unanimity now exists in the literature. The commonest adsorbed form consists of CO *terminally* bonded to single surface atoms in the plane, and this form is generally prevalent at high coverages on those metals that do not dissociatively adsorb CO. At lower coverages, differently ordered structures are possible, and evidence for these various structures has come from a variety of techniques.

LEED has now developed to the point where good agreement between experimental patterns and those calculated from the correct structural model may be anticipated, and fig.[25] shows both experimental data and the result of model calculations for Ni{001}c(2x2)-CO[51].

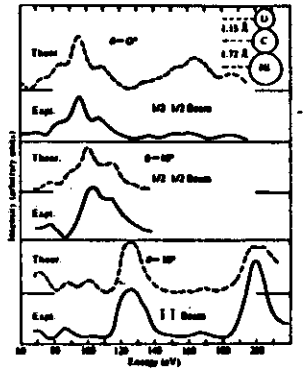

Fig.[25]. Comparison of the experimental and theoretical LEED spectra from Ni{001}c(2x2)-CO. The structural model is shown schematically at the top.[51]

The high oscillator strength associated with ν(C≡O)in the IR has led to the extensive exploitation of vibrational spectroscopy in the study of CO adsorption, and some results for the adsorption of CO on polycrystalline Rh particles on Al_2O_3 are shown in fig.[26][52] . The IR spectra show four peaks:

(a) a broad peak at 1866 cm^{-1} that shifts to 1870 cm^{-1} at maxmimum uptake,
(b) a weak band that shifts from 2050 to 2070 cm^{-1} as the coverage increases,
(c) an intense doublet at 2101 and 2031 cm^{-1} whose frequencies are coverage independent.

There are two observations that call for particular comment:

(1) Why do bands (a) and (b) shift to higher frequency with coverage?
(2) What are the origins of the bands?

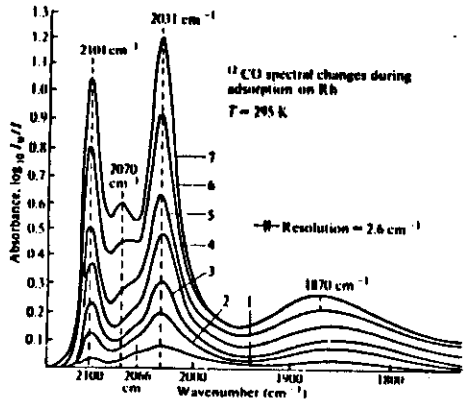

Fig.[26]. IR spectra for ^{12}CO adsorbed on rhodium for increasing CO coverage (T = 295 K): curve 1, $p_{CO} = 2.9 \times 10^{-3}$ torr; curve 2, $p_{CO} = 4.3 \times 10^{-3}$ torr; curve 3, $p_{CO} = 5.0 \times 10^{-3}$ torr; curve 4, $p_{CO} = 8.3 \times 10^{-3}$ torr; curve 5, $p_{CO} = 0.76$ torr; curve 6, $p_{CO} = 9.4$ torr; curve 7, $p_{CO} = 50$ torr.[52]

The assignment of the bands is strightforward:

(a) is derived from CO adsorbed at *binary* sites

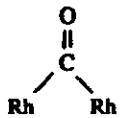

(b) is derived from CO adsorbed at *single* sites

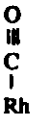

(c) is derived from individual atoms of Rh on the Al_2O_3 that can coordinate *two* carbonyls:

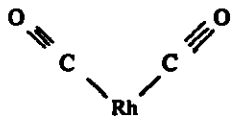

The shift of (a) and (b) was thought originally to be associated with the increased demands on the metal d_π donor orbitals. Back donation of these to CO reduces ν(C≡O), but as coverage increases, so does competition for the d_π orbitals and these therefore become less effective in terms of individual back-bonding. PLausible though this analysis is, it now appears

not to be the whole story, and dipole-dipole interactions also play an important role. Very similar shifts in the frequency of terminally bonded CO have been observed for CO on Pt(111) as shown in fig.[27][53].

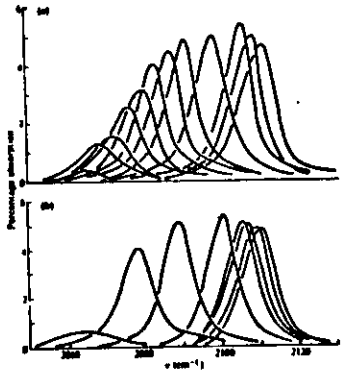

Fig.[27]. Reflection-absorption IR spectra for CO on Pt(111) at (a) 120 K and (b) 200 K. The band grows in intensity up to θ = 1/3 but is constant at higher coverages.[53]

For Pd(100) and $\theta_{CO} < 0.5$, a single peak is observed that shifts from 1895 cm^{-1} at low coverage to 1949 cm^{-1} at $\theta_{CO} = 0.5$. This peak is associated with *bridge* bonded CO and a structure proposed by Ertl[54] is shown in fig.[28].

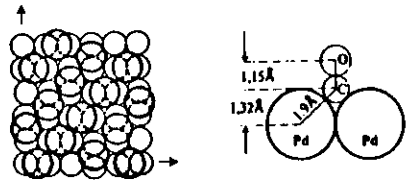

Fig.[28]. Structural model for CO adsorbed on palladium (100). The CO occupies bridging sites and gives a $(2\sqrt{2} \times \sqrt{2})R45°$ structure for which $\theta_{CO} = 0.5$.[54]

For CO adsorption on Rh(111) the absorption frequencies vary with coverage as shown in fig.[29].[55] Clearly, the principal peak, at 1990 cm^{-1}, shifts to higher frequency with coverage, reaching a limit of 2070 cm^{-1} at very high coverage (not shown). There is also a peak that has a frequency of 480 cm^{-1} at low coverage and which shifts down in frequency with increasing coverage, eventually reaching 420 cm^{-1}. In addition, a shoulder appears on the higher frequency band at 1870 cm^{-1}, and this does not shift with coverage. Once again, the 1990/2070 cm^{-1} peak is derived from a linearly bonded CO and the 1870 cm^{-1} peak is due to bridge bonding CO. The 480/420 cm^{-1} band is associated with the Rh-C stretch,

and it is interesting that the reduction of the d_π backbonding evident in the ν(C≡O) increase also leads to a lowering of the bond order of the M-C bond and this is the origin of the decreasing frequency.

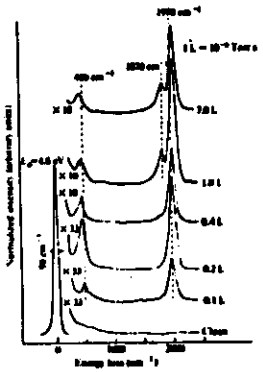

Fig.[29]. Vibrational spectra of CO chemisorbed on an initially clean rhodium (111) single-crystal surface at 300 K as a function of gas exposure.[55]

The adsorption of CO on Pd(111) shows how different ordered structures can evolve into one another. At θ = 1/3, the structure shown in fig.[30a] is postulated in which CO is *triply* bonded, with a very low stretching frequency of 1823 cm^{-1}. If this structure is compressed, it evolves to that of fig.[30b], in which the CO are *doubly* bridging. The coverage is now 0.5 and the stretching frequency 1936 cm^{-1}. This coverage is the highest that can be attained at room temperature, but cooling results in further adsorption to give the highly compressed structure of fig.[30c] with both triply and linearly bonded forms. The ease with which these films re-organise suggests that CO must be highly mobile on the surface of metals, and this is consistent with ^{13}C nmr results on carbonyl clusters.

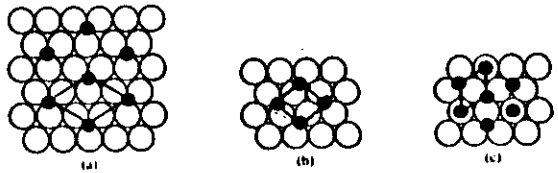

Fig.[30]. Models for the adsorption of CO on palladium (111): (a) a (√3x√3)R30° structure at θ_{CO} = 1/3; (b) a c(2x4) structure at θ_{CO} = 0.5 and (c) a hexagonal structure at θ_{CO} = 0.66.[56]

The bonding of terminal CO has also been explored by UV-PES, and the major shift in electronic energy level on adsorption takes place in the 5σ (*ie* carbon lone pair) orbital. It can be seen from fig.[31] that this 5σ level is well separated from the 1π level in the free molecule, but on adsorption this orbital becomes accidentally degenerate with the 1π

level[57], a result similar to that found for CO on Pd(110)[58].

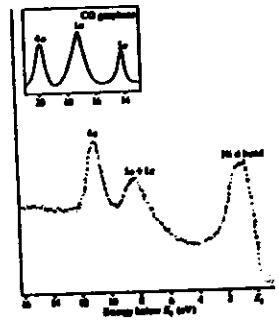

Fig.[31]. UV-PE Spectrum for CO adsorbed on Ni(100) at θ = 0.6[57]

Dissociative adsorption of CO is of prime importance in understanding certain mechanisms, and has been explored using X-PE Spectroscopy. An interesting example is iron: at low temperatures, on Fe(100), the UV-PE spectrum of adsorbed CO is typical of terminally bonded molecular CO with a pronounced differential shift of the 5σ orbital. Similar behaviour is also encountered in polycrystalline Fe, and a study by X-PES shows a C 1s peak characteristic of molecularly adsorbed CO, provided adsorption takes place well below room temperature. However, if such an adsorbed layer is heated above 350 K, the C 1s signal of molecular CO vanishes and is replaced by one characteristic of adsorbed carbon *atoms*[59]. Further investigation along these lines has suggested that dissociative chemisorption is typically found on metals where $-\Delta H_{ads} > ca.$ 250 kJ mol^{-1}. Iron, with $-\Delta H_{ads} \approx$ 180 kJ mol^{-1}, is clearly borderline.

Adsorption of CO on oxides

On oxides, unlike metals, the frequency of the CO band may be shifted to *higher* frequency[60,61]. The absorption frequency of CO in the gas phase is 2143 cm^{-1} and these reaches 2174, 2187 cm^{-1} on V^{3+}/SiO_2, where the suggested geometry of the surface site is[62]

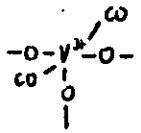

and 2185 cm^{-1} on TiO_2[63]. Interestingly, another peak, at 2115 cm^{-1}, can be seen on TiO_2, which has been ascribed to some form of CO acting as an intermediate in the formation of surface adsorbed HCO_3^-. Adsorption of CO on NiO has been extensively studied[64], and the following have been identified as species formed under various conditions:

frequency /cm^{-1}	species
2125, 2075	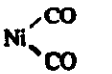 and/or $Ni(CO)_3$
1970	Ni–CO
1910, 1880	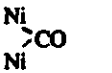 and/or Ni–CO
1730, 1160	organic-like carbonate
1655, 1533, 1280	bulk carbonate
1630, 1318	bidentate carbonate
1580, 1370	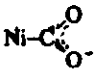
1470	monodentate carbonate
1215	hydrogen carbonate

Finally, CO adsorbed on ZnO has been reported to have a frequency of 2212 cm^{-1}[65]. As a rule of thumb, it has been suggested that M^{2+}–CO will have a stretching frequency in excess of 2170 cm^{-1}, M^{+}–CO will lie between 2120 and 2160 cm^{-1} and M^{o}–CO will lie below 2100 cm^{-1}.

II. Kinetics and Mechanism in catalysis: I Fundamentals

We shall first examine some of the ways in which the basic processes occurring at the surface can be described and the reactions formulated. The most straightforward models that have been suggested are the Langmuir-Hinshelwood mechanism, which envisages the reaction as taking place solely between surface adsorbed species, and the Eley-Rideal mechanism, which permits the involvement of both surface and gas-phase species in the overall reaction.

A. The Langmuir-Hinshelwood mechanism

The main assumptions are:

(i) The surface reaction is rate-limiting
(ii) The Langmuir isotherm can be applied to describe the equilibrium between the gas phase and adsorbed reactants and, where necessary, products.
(iii) The adsorbed reactants *compete* for surface sites.

(a) Unimolecular decomposition processes

The basic reaction is $A_{(gas)} \leftrightarrow A_{ads} \rightarrow B_{(gas)}$

and the rate of reaction $v = k'\theta_A = k'K_Ap_A/[1 + K_Ap_A]$

where k' is a heterogeneous rate constant and K_A is the Langmuir constant for gas A. There are two extreme cases:

(1) If $K_Ap_A \ll 1$, then $v \approx k'K_Ap_A = k_{exp}p_A$ and is first-order in the gas pressure

(2) If $Kp_A \gg 1$, then $v = k'$ and is zeroth order in gas pressure

In case 1, the temperature dependence of the experimental rate constant is

$$\partial(\ln k_{exp})/\partial T = (E' + \Delta H_{ads})/RT^2 = E_{exp}/RT^2$$

where E' is the activation energy for the heterogeneous reaction on the surface. Note that $E_{exp} < E'$ since $\Delta H_{ads} < 0$. The overall activation energy is, therefore, lowered.

If B is adsorbed and competes with A for sites on the surface, then:

$$A_{(gas)} \leftrightarrow A_{ads} \rightarrow B_{ads} \leftrightarrow B_{(gas)}$$

and, from a simple extension of the Langmuir isotherm,

$$\theta_A = \frac{K_Ap_A}{1 + K_Ap_A + K_Bp_B}$$

If $K_Ap_A \ll 1 + k_Bp_B$, $v \approx k'K_Ap_A/[1 + k_Bp_B]$

$= k'K_Ap_A/k_Bp_B$ if $k_Bp_B \gg 1$

(b) Bimolecular surface reactions

These have the general mechanistic form:

$$\begin{array}{ll} A_{(gas)} & B_{(gas)} \\ \uparrow\downarrow & \uparrow\downarrow \end{array}$$

$$A_{ads} + B_{ads} \rightarrow C_{(gas)}$$

and from the above we see immediately that

$$v = \frac{k'K_AP_AK_BP_B}{(1 + K_AP_A + K_BP_B)^2}$$

If K_A, K_B are <u>comparable</u>, then v will go through a <u>maximum</u> as p_B is increased whilst p_A is fixed. If, by contrast, K_AP_A, $K_BP_B \ll 1$, then

$$v \approx k_{exp}P_AP_B$$

and is second order in gas-phase pressures. If A is weakly adsorbed so that $K_AP_A \ll K_BP_B + 1$, then

$$v \approx \frac{k'K_AP_AK_BP_B}{(1 + K_BP_B)^2}$$

which is first order in A. If B is <u>strongly</u> adsorbed in this case, so that $K_BP_B \gg 1$, then

$$v \approx (k'K_A/K_B).P_A/P_B - k_{exp}P_A/P_B$$

and the reaction is <u>inhibited</u> by B. The activation energy is given by

$$E_{exp} = E' + \Delta H_{(ads)A} - \Delta H_{(ads)B} > E'$$

since $-\Delta H_{(ads)A} < -\Delta H_{(ads)B}$. Thus, if one of the reactants is strongly <u>adsorbed</u>, the reaction is slowed down.

If C (the product of A & B) is also adsorbed, then

$$v = k'\theta_A\theta_B = \frac{k'K_AP_AK_BP_B}{(1 + K_AP_A + K_BP_B + K_CP_C)^2}$$

and if C is <u>strongly</u> adsorbed, such that $K_CP_C \gg 1 + K_AP_A + K_BP_B$, then

$$v \approx (k'K_AK_B/K_C^2).P_AP_B/P_C^2$$

and the rate is strongly inhibited by the product.

B. <u>The Eley-Rideal Mechanism</u>

The main distinction from the langmuir-Hinshelwood mechanism is in assumption (i) above, which is replaced by the possibility of reaction between adsorbed and gas-phase species as:

$$A_{ads} + B_{(gas)} \rightarrow \text{products}$$

whence the reaction velocity is

$$v = k''\theta_AP_B = k''K_AP_AP_B/[1 + K_AP_A]$$

and the major kinetic distinction lies in the behaviour is p_A is kept constant and p_B is increased. In the corresponding Langmuir-Hinshelwood expression, it is seen that the rate will go through a maximum, whereas the Eley-Rideal expression predicts an increase without limit.

<u>Variation of catalytic rate with temperature</u>

We have seen that Arrhenius behaviour is expected in certain of the cases quoted above, but in other cases the reaction rate may actually go through a maximum as T increases. Physically, this is because there is a tendency for surface coverage to <u>decrease</u> at higher temperatures. This may be seen graphically by considering the Langmuir-Hinshelwood model for the bimolecular process above for which

$$v = \frac{k'K_AP_AK_BP_B}{(1 + K_AP_A + K_BP_B)^2}$$

Now, if, at low temperatures, $K_BP_B \gg 1 + K_AP_A$, $v \sim (k'K_A/K_B).P_A/P_B$ and the activation energy

$$E_{exp} = E' + \Delta H_{(ads)A} - \Delta H_{(ads)B} > 0$$

so that at low temperatures, the Arrhenius slope will be normal and the reaction will show an increase with temperature. At higher temperatures, we will suppose that K_B has decreased to the point where K_BP_B, $K_AP_A \ll 1$ and

$$v \approx k'K_AP_AK_BP_B$$

The activation energy is now

$$E_{exp} = E' + \Delta H_{(ads)A} + \Delta H_{(ads)B}$$

and it is perfectly possible that E_{exp} will become <u>negative</u>, and the reaction rate <u>decrease</u> with T. From this analysis, it is clear that the reaction rate will actually go through a maximum as the temperature is increased.

If, in a bimolecular reaction, the product C is strongly adsorbed at lower temperatures, then increasing the temperature will always increase the rate. However, the rate may remain very low until the temperature is reached at which flash desorption begins, in which case it will rise steeply. Above this point, it may remain relatively independent of T since

the rate will now depend on the sticking fraction, which, as we saw above, is not a strong function of temperature in many cases. One well-known example is the isotopic scrambling of CO, and results for Re are shown in fig.[32][66]

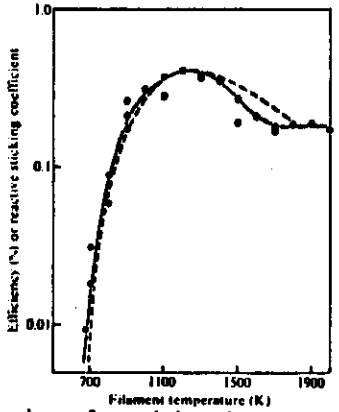

Fig.[32]. A comparison of two independent measurements of the efficiency of rhenium as a catalyst for the isotope reaction $^{12}C^{18}O + {}^{13}C^{16}O \rightarrow {}^{12}C^{16}O + {}^{13}C^{18}O$ [66].

51. M. Passler, A. Ignatiev, F.P. Jona, D.W. Jepson and P.M. Marcus
Phys. Rev. Lett. 43 (1979) 360
52. J.T. Yates, T.M. Duncan, S.D. Worley and R. Vaughan
J. Chem. Phys. 70 (1979) 1219
53. R.A. Shigeishi and D.A. King
Surf. Sci. 58 (1976) 379
54. G. Ertl
Pure Appl. Chem. 52 (1980) 2051
55. L.H. Dubois and G.A. Samorjai
"Vibrational Spectroscopies for Adsorbed Species", eds. A.T. Bell and M.L. Hair, A.C.S. Symposium Ser. 137 (1980)
56. H. Conrad, G. Ertl and J. Küppers
Surf. Sci. 76 (1978) 323
57. A.M. Bradshaw
Surf. Sci. 80 (1979) 215
58. J. Küppers, H. Conrad, G. Ertl and E.E. Latta
Jap. J. Appl. Phys. Supp. 2(2) (1974) 225
59. M.W. Roberts
Chem. Soc. Rev. 6 (1977) 373
60. J.B. Peri
J. Catal. 86 (1984) 89
61. N.S. Hush and M.L. Williams
J. Mol. Spec. 50 (1974) 349
62. B. Rebenstorf, M. Berglund and R. Lykvist
Z. Phys. Chem. N.F. 126 (1974) 349
63. K. Tanaka and J.W. White
J. Phys. Chem. 86 (1982) 4708
64. E. Guglielminotti, L. Ceruti and E. Borello
Gazz. Chim. Ital. 107 (1977) 503
65. C.H. Amberg and D.A. Seanor
Proc. 3rd. Int. Cong. Catal., Amsterdam, 1965, p.450
66. R.P.H. Gasser and D.E. Holt
Surf. Sci. 63 (1977) 520

Lecture 5

Fundamentals of Catalysis II

Variation of Catalytic Rate with Substrate

The basic process of catalysis is shown in fig.[33] and it is clear that the steps that may be activated are:

(i) chemisorption
(ii) the heterogeneous reaction
(iii) desorption

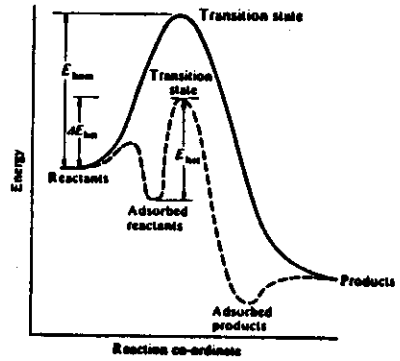

Fig.[33]. Schematic representation of the transition state theory of a homogeneous reaction (———) and a heterogeneous reaction (--------)[6].

It can be seen that if the chemisorption is weak, surface coverage will be low and catalytic activity also low. As $-\Delta H_{ads}$ increases, the coverage will rise, but so may E*j*. At large enough values of $-\Delta H_{ads}$, the coverage will reach a limiting value, but E*j* may now be so large that the adsorbed species cannot be decomposed; catalytic activity will again be low. Thus, there will, in general, be an optimal chemisorption strength as shown in fig.[34].

We may vary ΔH_{ads} by varying the substrate, and we therefore expect that a plot of catalytic activity *vs.* position of catalyst in the periodic table may also show a maximum. This is illustrated in fig.[35] for the hydrogenation of ethene, which is believed to be a Langmuir-Hinshelwood type bimolecular process with C_2H_4 strongly chemisorbed.

If adsorption energy can be estimated, then the type of plot shown in fig.[35] may be converted to a true "volcano" plot by displaying rate as a function of an enthalpy term. One elegant example is the rate of decomposition of formic acid. This chemisorbs very strongly on metals to form a surface formate species, so the enthalpy of formation of the metal formate may be taken as a measure of ΔH_{ads}. If the rate of the reaction is plotted as the temperature T_r at which the rate reaches a fixed value, then

the volcano plot of fig.[36] results[67]. Note that in fig[36], T_r is plotted down the axis.

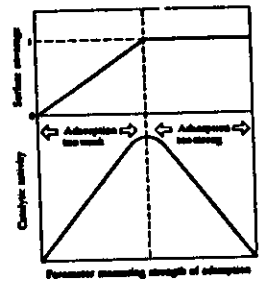

Fig.[34]. The "volcano" curve; dependence of catalytic activity on strength of reactant adsorption (lower part) and the corresponding variation in surface coverage (upper part)[26]

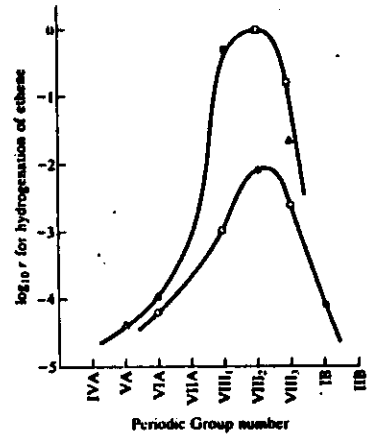

Fig.[35]. Logarithm of the rate of hydrogenation of ethene relative to that found on rhodium *vs.* periodic table group number. Open points: evaporated metal films; filled points: silica-supported metals. Circles: first transition series; squares: second and triangles third series.[26]

Experimental Distinction between Langmuir-Hinshelwood and Eley-Rideal Mechanisms

Immense efforts have been made in recent years to distinguish between these two mechanisms experimentally, and there are two broad categories of approach. In the first, a steady state is established by flowing gas mixtures over the catalyst, and then the temperature of the catalyst or pressures of the reacting gases are varied systematically. A second approach is to establish conditions remote from steady state by making abrupt changes in one or more variables and then to monitor the relaxation of the system.

To focus discussion, we consider the oxidation of CO on palladium. Two mechanisms have been proposed[68], based on the Langmuir-Hinshelwood and Eley-Rideal models.

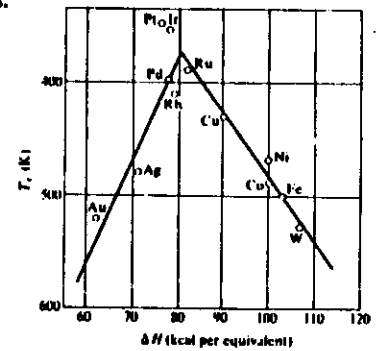

Fig.[36]. The rate of decomposition of formate, plotted as T_r, *vs.* the enthalpy of formation of the metal formate salt[67].

(i) Langmuir-Hinshelwood Mechanism

$$CO_{(gas)} \rightarrow CO_{ads} : k_1$$
$$CO_{ads} \rightarrow CO_{(gas)} : k_2$$
$$O_2(g) \rightarrow 2O^{\cdot}_{ads} : k_3$$
$$CO_{ads} + O^{\cdot}_{ads} \rightarrow CO_2(gas) : k_4$$

(ii) Eley-Rideal Mechanism

$$O_2(gas) \rightarrow 2O^{\cdot}_{ads} : k_3$$
$$O^{\cdot}_{ads} + CO_{(gas)} \rightarrow CO_2(g) : k_5$$

Although a number of steady state techniques has been deployed to distinguish these mechanisms, the most powerful tool has been the use of modulated molecular beams. In this experiment, one gas is flowed through at a steady pressure, and the other gas is in the form of a molecular beam that can be modulated by a shutter at a frequency of 100 – 1000 Hz. Thus, for oxidation of CO on Pd(111), a modulated beam of CO can be used, and the CO_2 formed detected mass spectrometrically. In addition to delays between opening the shutter and the detection of CO_2 that can be attributed to purely kinematic effects, there will be an additional delay occasioned by the finite rate of the surface reaction. Let this additional delay be represented by a phase lag ϕ. Then ϕ will be a strong function of the mechanism. If the CO beam is modulated, and conditions fixed such that θ_{CO} is small (≤ 0.03) and coverage by atomic oxygen large ($\theta_O > 0.1$), then we find[68]:

$$\partial[CO_2]/\partial t = k_4\theta_{CO}\theta_O \qquad \text{(L-H mechanism)}$$

$$\partial[CO_2]/\partial t = k_5\theta_{CO}\theta_O \qquad \text{(E-R mechanism)}$$

where we have approximated the rather complex functional dependence of the experimental rate law on O coverage.

Let now the modulation of the beam be described in terms of the modulation of the pressure of CO, such that

$$p_{CO} = p^{o}_{CO} + \alpha e^{i\omega t}$$

then

$$\theta_{CO} = \theta^{o}_{CO} + \beta e^{i\omega t}$$

For the L-H mechanism, inserting these expressions for p_{CO} and θ_{CO} into the rate law for θ:

$$\partial\theta_{CO}/\partial t = k_1 p_{CO} - k_2\theta_{CO} - k_4\theta_{CO}\theta_O$$

we obtain, retaining just harmonic terms

$$i\omega\beta = k_1\alpha - k_2\beta - k_4\beta\theta_O$$

whence

$$\beta = k_1\alpha e^{-i\phi}/([k_2 + k_4\theta_O]^2 + \omega^2)^{1/2}$$

where

$$\tan\phi = \omega/[k_2 + k_4\theta_O]$$

The final expression for the rate of production of CO_2 in the L-H model is then

$$\partial[CO_2]/\partial t = k_4\theta_O\left\{\theta^{o}_{CO} + \frac{k_1\alpha e^{i(\omega t - \phi)}}{([k_2 + k_4\theta_O]^2 + \omega^2)^{1/2}}\right\}$$

In a similar way, the E-R mechanism yields

$$\partial[CO_2]/\partial t = k_5\theta_O\{p^{o}_{CO} + \alpha e^{i\omega t}\}$$

and $\tan\phi = 0$

Thus, for the L-H mechanism, $\tan\phi$ is predicted to be temperature dependent through the rate constants k_2 and k_4 whereas for the E-R mechanism, $\tan\phi$ is independent of T. The results shown in fig.[37] for CO on Pd(111) shown without any doubt that the L-H mechanism holds. In fact, inder the conditions of the experiment, $k_2 \gg k_4\theta_O$, so $\tan\phi \approx \omega/k_2$ and a plot of $-\ln\tau \equiv -\ln(1/k_2)$ vs. $1/T$ gives the activation energy for desorption as 139 kJ mol^{-1}. This is very close to the isosteric heat of adsorption of CO on Pd(111) since adsorption of CO is not activated. The activation energy for k_4 may be obtained by plotting the CO_2 signal at a fixed ω vs. T, since, with the approximations above, the phase-detected signal is given by const.$k_4/[k_2^2 + \omega^2]^{1/2}$. This gives the activation energy for k_4 as 105 kJ mol^{-1}.

Mass Transport Limitations on catalysis

It is clear that any heterogeneous catalytic process must involve five basic steps:

(1) Transport of reactants to the surface
(2) Adsorption of the reactants on the catalyst
(3) Reaction on the catalyst involving one or more adsorbed species
(4) Desorption of the products
(5) Transport of products away from the catalyst.

Hitherto we have not considered the mass transport processes, and indeed for many gas phase reactions on simple catalysts these processes are not rate limiting. however, at low pressures, or in the use of porous or reticulated catalytic supports, mass transport may become limiting. The problem of mass transport in liquid/solid systems is far more serious since diffusion coefficients are very much lower in the liquid than in the gas phase.

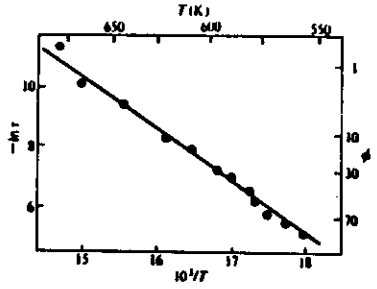

Fig.[37]. Arrhenius plot of $-\ln\tau \equiv -\ln(1/k_2)$ vs. 1/T for CO oxidation on Pd(111). The modulation frequency was 779 Hz.[68].

For porous catalyst supports or particles, the determination of whether the reaction is transport limited often presents a significant experimental problem, since stirring or agitation of the fluid will have only a marginal effect. The optimisation of catalyst design is a complex multivariate problem, requiring advanced statistical techniques, and is beyond the scope of this lecture course. However, one important effect may be that a transition can occur from a low-temperature régime in the the rate is dominated by heterogeneous effects and has an associated activation energy that is quite large, and a high-temperature régime in which diffusion effects dominate and the activation energy falls considerably. There is a number of possible origins of this effect when it is found experimentally, but transport limitation is an important one.

Branching

The simple situations envisaged at the beginning of this lecture are rarely encountered in practice. Much more common are processes in which branching or sequential mechanisms are operative. Three typical examples are:

I: $A + B \nearrow C$, $B \searrow D$

II: $A + B \rightarrow C \rightarrow D$

III: $A + B \nearrow C \downarrow D$, $B \searrow D$

The selectivity for a particular product i can be defined as

$$S_i = \xi_i/(\Sigma_j \xi_j)$$

where the ξ_i are the rates of formation of i. The selectivity can be contrasted with the conversion which is defined as the fraction of reactant converted into all the products. For the three mechanisms given above, plots of selectivity for C, S_C, and yield of the products C and D *vs.* conversion are shown in fig.[38].

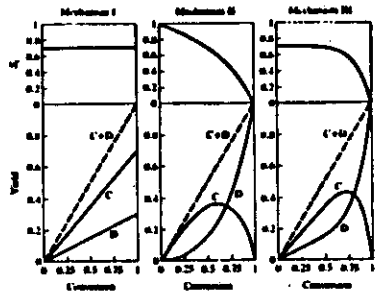

Fig.[38]. Variation of the yields of the products C and D with conversion of reactants according to the mechanisms I – III above (lower part of each graph) and variation of selectivity for the intermediate product C (S_C) with conversion (upper curves)[26].

The Fischer-Tropsch Process

We conclude this lecture course by an examination of one of the most fascinating of the heterogeneously catalysed reactions of CO, the Fischer-Tropsch reaction, which involves the conversion of mixtures of CO and H_2 into awide range of hydrocarbon derivatives.

Historically, the first report of the hydrogenation of CO to give liquid hydrocarbons was in 1916 by the Badische Anilin u. Soda Fabrik, the catalyst being Co metal and the conditions severe (100 atm./300-400 °C). Later investigations at the Kaiser Wilhelm Institut für Kohleforschung at Mühlheim/Ruhr by Fischer and Tropsch established that much milder

conditions (1 atm./250 - 350 °C) could be used with mixed Fe or Co catalysts, though these were rapidly poisoned by sulphur. Industrial scale-up, using Co/ThO_2 catalysts and CO from coal was plagued by technological problems, though it was sufficiently successful in the end that, by 1941, nine Fischer-Tropsch plants were in operation. However, in the post-war period, the availability of cheap petroleum led to the abandonment of coal-based F.T. plants save in countries where special economic circumstances prevailed.

Catalysts for the general processes:

$$nCO + 2nH_2 \longrightarrow -(CH_2)_n- + nH_2O$$: favoured by Co

and

$$2nCO + nH_2 \longrightarrow -(CH_2)_n- + nCO_2$$: favoured by Fe

include Fe, Co, Ni, Ru, and ThO_2, with Fe being currently preferred. The active surface phase remains controversial, with metallic or metal-like components (such as nitrides or carbides) playing an important role for Ni, Co and Ru. The case of Fe is more complex as dynamic modification to the surface occurs, with formation of mixed phases such as oxides and carbides. Each catalyst tends to produce different mixtures as shown in fig.[39], with some of the mixtures being very complex, particularly with Fe. The main point is that, by and large, straight chain or methyl-branched isomers are produced, but more highly branched alkanes are not formed in significant quantities.

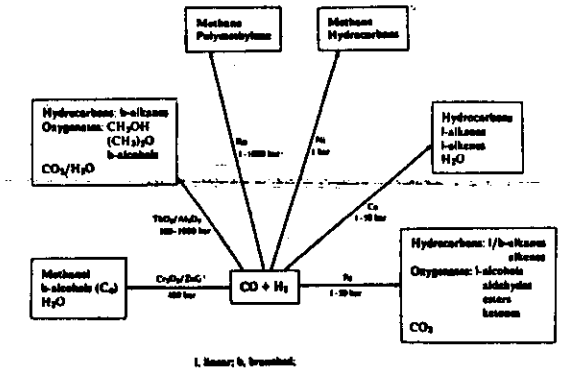

l, linear; b, branched.

Fig.[39]. Products of hydrocondensation of CO on different catalysts[69].

Basic Mechanisms

The essential processes that must take place are:

1: Scission of the original C≡O bond
2: Formation of new C–C, C–H, and C–O bonds
3: Formation of surface carbides and carbon itself

It appears that the first step is the dissociative chemisorption of CO which is known to take place on ironand believed to ocur also on Co and Ni under the appropriate conditions. In the presence of hydrogen, however, these adosrbed carbon atoms will react, and a surface equilibrium mixture of CH_x will form, with x in the range 0–2. On Nickel catalysts, the reaction of these CH_x species is believed to take place with each other through a chain growth mechanism of the general sort:

and from studies with isotopically labelled CO, these oxygen-free species appear to act both as initiators and propagators. The weight of evidence is now that the dominant species on nickel is CH_2, and the basic mechanism is thought to be:

$$RCH_2\text{–}M + CH_2M' \rightarrow RCH_2CH_2M' + M$$: propagation

$$RCH_2\text{–}M + CH_3M' \rightarrow RCH_3 + M + CH_2M'$$: termination

$$RCH_2M + CH_3M' \rightarrow M + R'CH{=}CH_2 + H_2 + CH_2M'$$: termination

$$RCH_2\text{–}M + M'CO \rightarrow M + RCH_2COM' \rightarrow M + M' + RCH_2CH_2OH$$: termination

The methylene adsorbates may not be present on single sites, and one possibility is that they may occupy double Ni sites as

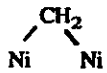

Some confirmation of the above scheme is provided by the observation that diazomethane, diluted by He or N_2, is converted on a Ni surface to ethene but in the presence of H_2, the products are a mixture of linear C_1 to at least C_{18} alkanes and alkenes, similar to those obtained with CO/H_2 feedstock.

We have seen that CO may intervene in the chain propagation process to yield alchohols. In fact, aldehydes and carboxylates could also be produced as

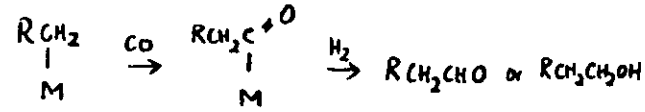

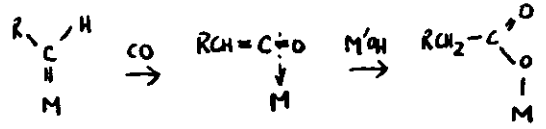

and this process may be highly significant on Fe. In the case of Fe, the processes are very complex, and are schematically indicated in fig.[40].

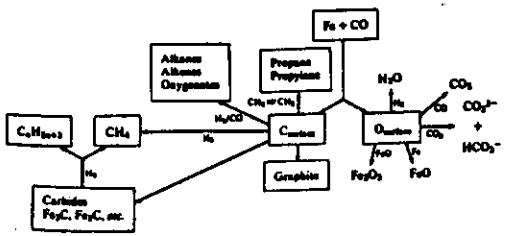

Fig.[40]. Possible evolution of $C_{surface}$ and $O_{surface}$ in F.T. synthesis.

In this scheme, graphite represents a poison, inert to H_2 under the conditions of the catalysis, but the carbidic phase, which represents a complex mixture of iron carbides, does react with hydrogen to give CH_4 and other hydrocarbon products. Some support for the reactivity of C attached to iron is seen from the model reactions involving the iron carbonyl cluster $[(Et_4N)_2Fe_6C(CO)_{16}]^{2-}$ which can be oxidatively cleaved to yield a Fe_4 cluster as:

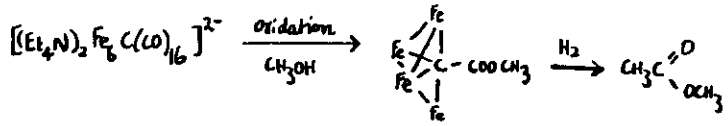

In the case of Ru, conditions can be adjusted to give polymethylene with quite high molecular weight (5000 - 23000). Again, the reaction is believed to proceed by methylene adsorbed on the surface. Growth may be te mechanism indicate above, or by CH_2 insertion as

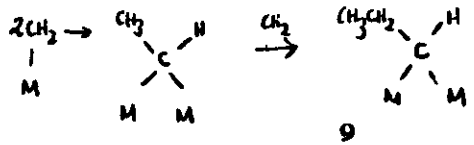

or CH_2 coupling as:

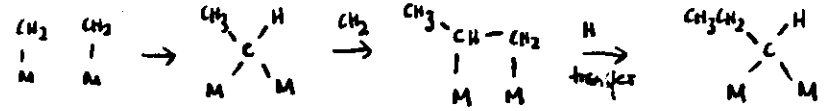

and

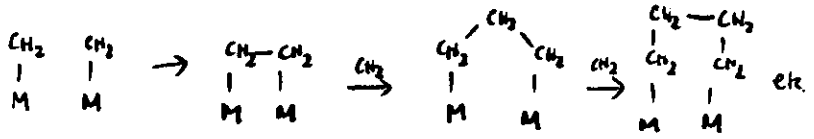

67. W.J.M. Rootsaert and W.M.H. Sachtler
Z. Phys. Chem. N.F. 26 (1960) 16
68. T. Engel and G. Ertl
J. Chem. Phys. 69 (1978) 1267
69. "Comprehensive Organometallic Chemistry", 8